Hidden-crossing mechanism of rotational excitation of H_2O by electric pulse

2004 J. Phys. B: At. Mol. Opt. Phys. 37 3419

(http://iopscience.iop.org/0953-4075/37/17/003)

INSTITUTE OF PHYSICS PUBLISHING JOURNAL OF PHYSICS B: ATOMIC, MOLECULAR AND OPTICAL PHYSICS

J. Phys. B: At. Mol. Opt. Phys. **37** (2004) 3419–3426 PII: S0953-4075(04)80496-6

Hidden-crossing mechanism of rotational excitation of H_2O by electric pulse

G V Mil'nikov[1], H Nakamura[1,2] and E A Solov'ev[1,3]

[1] Department of Theoretical Studies, Institute for Molecular Science, Myodaiji, Okazaki 444-8585, Japan
[2] Department of Functional Molecular Science, The Graduate University for Advanced Studies, Myodaiji, Okazaki 444-8585, Japan
[3] Macedonian Academy of Sciences and Arts, PO Box 428, 1000 Skopje, Macedonia

E-mail: solovev@manu.edu.mk

Received 7 May 2004
Published 17 August 2004
Online at stacks.iop.org/JPhysB/37/3419
doi:10.1088/0953-4075/37/17/003

Abstract

Rotational excitation of the water molecule by an electric pulse $F(t)$ of Gaussian shape is studied in the framework of the adiabatic approach. The hidden crossings between rotational energy surfaces of H_2O in the complex F-plane are calculated by describing H_2O as an asymmetric-top rotor with electric dipole moment. It is found that the probabilities of the transitions oscillate uniformly with respect to the length of the pulse due to the interference between elementary transitions via hidden crossings during increasing and decreasing stages of the pulse. For a long pulse, the transition probabilities obtained in the adiabatic approximation are in good agreement with the exact numerical results: the longer the pulse the better the agreement.

1. Introduction

We consider the H_2O molecule because of its extraordinary role in living matter. Recently, the transition between collective rotational states of the water molecules in the brain cell were proposed as a possible mechanism for memory imprinting [1]. The hidden-crossing analysis of the rotational transitions shows that the transitions, induced by nervous signals, transfer the information rather than the energy, because the transition probability depends on frequency and does not depend on the amplitude of the signal [1]. Besides, the number of water molecules in the brain cell can be estimated by the efficiency of the interaction of the cell with the nervous signal. At the typical frequency of the nervous signal $\sim$10 Hz, this number is obtained to be very close to the actual number of water molecules in the brain cell [1].

The first application of the adiabatic approach to the transitions between rotational energy levels of H_2O induced by an electric pulse $F(t)$ was done using the model of the spherical rotor

having an electric dipole moment [2]. In the adiabatic approach, the branch points F_c of the adiabatic energy surface $E_N(F) \sim \sqrt{F - F_c}$ in the complex plane of adiabatic parameter F are responsible for the inelastic transitions [3]. Generally, there are two types of branch points connecting the adiabatic states. The first type is the branch points near the real axis which manifest themselves as narrow avoided crossings at the real value of the adiabatic parameter. Usually, the narrow avoided crossings appear due to the resonant underbarrier interaction of the states located in different potential wells. The second type is the branch points that have a large imaginary part. They are not recognizable on the plot of the adiabatic energy curves at real value of the adiabatic parameter, and appear when the adiabatic energy level touches the top of the effective potential. The calculations of rotational energies of a spherical rotor in an external electric field reveal a full set of the complex branch points F_c connecting pairwise the energy surfaces related to different energy levels at real F [2]. Since they are not visible at real values of F they were called hidden crossings, in analogy with atomic collision theory. For details, one can find the hidden-crossing theory in the review paper [4].

In this paper, we employ a much more realistic approach to the problem based on the Hamiltonian for the asymmetric-top rotor having an electric dipole moment. This model was used in the investigation of the energy level statistics for H_2O in strong electric fields [5] and for the calculation of inelastic transitions in collisions of positive ions with the water molecule [6]. Section 2 contains the numerical algorithm for the calculation of adiabatic energy surface and its branch points in the complex F-plane. In section 3, the adiabatic theory is described for the case of the double transitions via the same hidden crossing during increasing and decreasing stages of the pulse. In section 4, the transition probabilities from the ground state to the excited states obtained in the adiabatic approximation are compared with the *ab initio* numerical calculation of the corresponding non-stationary Schrödinger equation. Concluding remarks will follow in section 5.

Atomic units are used throughout, unless explicitly indicated otherwise.

2. H_2O as asymmetric-top rotor in electric field

The first vibrational excitation of H_2O lies 1596.5 cm^{-1} above the ground state [7]. Below this energy one can safely neglect the vibrational excitation and describe the molecular dynamics in the electric field $\boldsymbol{F}$ by the asymmetric-top model Hamiltonian

$$H = A J_a^2 + B J_b^2 + C J_c^2 - \boldsymbol{F}\boldsymbol{d} \tag{1}$$

where J_a, J_b and J_c are the components of the angular momentum along the principal axes in the body fixed frame (BF), and $\boldsymbol{d} = (d_a, d_b, d_c)$ is a constant electric dipole moment. The rotational transitions in the spherical rotor model ($A = B = C = 8.78 \times 10^{-5}$) were previously studied in [2]. In this work, we use realistic parameters for the H_2O molecule: $A = 1.27 \times 10^{-4}$, $B = 4.23 \times 10^{-5}$, $C = 6.62 \times 10^{-5}$ and $\boldsymbol{d} = (0, 0, 0.763)$ [8]. We assume that the external field is oriented along the z-direction in the space-fixed frame of reference (SF). In this case, the last term in the Hamiltonian is $d_c F \cos\beta$, where β is the Euler angle between the z-axes in BF and SF frames of reference. The Hamiltonian can now be represented by the corresponding finite-dimensional matrix within the basis of the normalized D-functions $|J, K, M\rangle$ [9]. Note that our notation differs from the usual order of the rotational constants $A > B > C$. We prefer to have the dipole moment oriented along the body-fixed z-axis which simplifies the calculations of the matrix elements. The free rotor part of the Hamiltonian is diagonal with respect to the total angular momentum J and its projection M

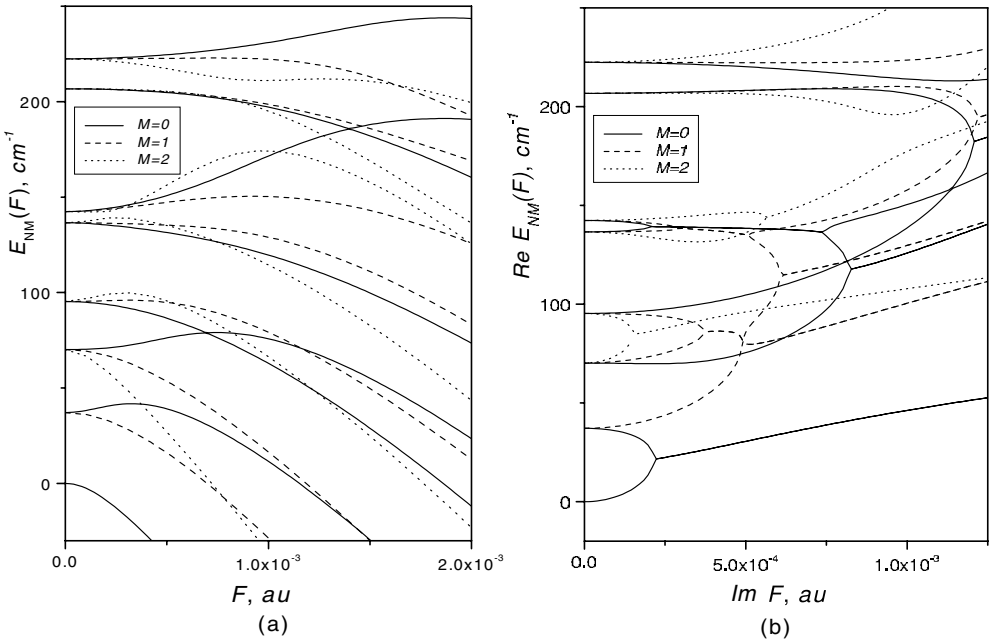

Figure 1. (a) The adiabatic energy curves $E_{NM}(F)$ for even K along the real axis of electric field F. (b) The real part of the energy curves $E_{NM}(F)$ for even K along the imaginary axis of electric field F.

onto the SF z-axis. For different K and K' values, the nonzero matrix elements are

$$\langle K|J_a^2|K\rangle = \langle K|J_b^2|K\rangle = \tfrac{1}{2}[J(J+1) - K^2], \qquad \langle K|J_c^2|K\rangle = K^2, \tag{2}$$

$$\langle K|J_a^2|K+2\rangle = \langle K+2|J_a^2|K\rangle = -\langle K|J_b^2|K+2\rangle = -\langle K+2|J_b^2|K\rangle$$
$$= \tfrac{1}{4}\sqrt{(J-K)(J-K-1)(J+K+1)(J+K+2)}. \tag{3}$$

The matrix of the dipole interaction $\cos\beta = |1, 0, 0\rangle$ is diagonal with respect to K, M, and it can be calculated from the D-function multiplication theorem as

$$\langle J|\cos\beta|J\rangle = \frac{KM}{J(J+1)}, \tag{4}$$

$$\langle J|\cos\beta|J+1\rangle = \frac{\sqrt{(J+K+1)(J-K+1)(J+M+1)(J-M+1)}}{(J+1)\sqrt{(2J+1)(2J+3)}}. \tag{5}$$

As follows from equations (2)–(5) the Hamiltonian has two exact quantum numbers: M and the parity of K. The latter corresponds to (A, B_z) (even K) and (B_x, B_y) (odd K) subspaces in the terminology of [5]. In the case $M = 0$, the matrix of dipole interaction (4), (5) does not depend on the sign of K, and the additional $(\pm)$ symmetry exists due to the disappearance of the interaction between the states $\{|J, K, M\rangle + |J, -K, M\rangle\}/\sqrt{2}$ and $\{|J, K, M\rangle - |J, -K, M\rangle\}/\sqrt{2}$ [6].

The ro-vibrational spectrum of the water molecule has been well studied both experimentally and theoretically (see [10] and references there). At $F = 0$ our rotational spectrum reproduces the experimental data [11] and accurate variational calculations [12, 13] within 0.3% level of accuracy. Figure 1 shows three noninteracting (A, B_z)

Table 1. Branch points $F_{NN'}$ between rotational states N and N' of H_2O within the manifolds $M = 0$, $M = 1$ and $M = 2$ having even value of K. $F_R = \mathrm{Re}\, F_{NN'} 10^4$ au and $F_I = \mathrm{Im}\, F_{NN'}$ 10^4 au.

	$M = 0$			$M = 1$			$M = 2$	
(N, N')	F_R	F_I	(N, N')	F_R	F_I	(N, N')	F_R	F_I
(1, 2)	0.00	2.15	(1, 2)	0.00	4.90	(1, 2)	0.00	1.50
[2]	0.00	2.18	(1, 2)	0.00	6.21	(1, 2)	0.00	11.5
(2, 3)	2.81	3.07	(2, 3)	0.00	3.71	(2, 3)	1.97	3.12
(3, 5)	0.00	8.18	(3, 4)	3.97	6.14	(3, 4)	2.22	0.66
(3, 6)	5.63	6.15	(3, 4)	0.00	6.06	(3, 4)	0.00	5.60
(5, 6)	0.00	7.45	(4, 5)	0.00	2.90	(4, 5)	1.16	9.21
(4, 7)	0.00	12.0	(4, 5)	0.00	5.11	(4, 5)	9.13	3.75
(6, 8)	4.11	12.0	(4, 5)	5.36	7.85	(5, 6)	8.10	2.80
(6, 8)	12.9	7.45	(5, 6)	6.69	10.1	(6, 7)	0.00	9.99
(6, 8)	0.32	16.7	(6, 7)	6.07	8.16	(6, 7)	8.05	8.00

families ($M = 0, 1, 2$) of the adiabatic energy curves $E_{NM}(F)$ as a function of the adiabatic parameter F, where $N = 1, 2, 3, \ldots$ numbers the states in order of the energy increasing at $F = 0$ in each M-family (see figure 1(a)). The sequence $N = 1 - M$, $2 - M$, $3 - M$, $4 - M$, $5 - M$, $6 - M$, $7 - M$, $8 - M$ (positive values of N have a physical meaning) corresponds to the sequence of the standard set of the quantum numbers $J_{K_a K_c} = 0_{00}, 1_{11}, 2_{02}, 2_{11}, 2_{20}, 3_{13}, 3_{22}, 3_{31}$, where K_a and K_c are the projections of the total angular momentum J onto principal axes A and C at the conventional option $A > B > C$ [13]. At real F (figure 1(a)), the main feature is the absence of any avoided crossings which usually serve as a trace of the branch points in the complex plane (one can only see exact crossings for $M = 0$ which are due to the $(\pm)$ symmetry mentioned above). However, the branch points related to the hidden crossings do exist and they can be revealed by direct numerical calculation in the complex F-plane. In figure 1(b), we depict the behaviour of the real part of the adiabatic energy $\mathrm{Re}\, E_{NM}(F)$ as a function of $\mathrm{Im}\, F$ along the imaginary axis $\mathrm{Re}\, F = 0$. Table 1 gives the distribution of the branch points in the complex F-plane. The first hidden crossing for the spherical rotor [2] in each series $M = 0, 1, 2$ is also presented. In the cases $M = 0$ and $M = 1$ we have reasonable agreement with the present data, but for $M = 2$ the spherical rotor does not reproduce the actual behaviour of the energy surface shown in figure 1(b). From the table one can see that many hidden crossings have real parts equal to zero and, in particular, the branch point between the ground state and the first excited state. This is a very important physical property: for such hidden crossings the inelastic transitions take place for arbitrarily small amplitude of the electric pulse and the transitions, induced by the periodic signal, transfer the information rather than the energy, because the transition probability depends on frequency and does not depend on the amplitude of the signal (see [1]).

3. Adiabatic approximation

The adiabatic approximation is an asymptotic solution of the non-stationary Schrödinger equation

$$H(F(vt))\psi(\boldsymbol{r}, t) = \mathrm{i}\frac{\partial \psi(\boldsymbol{r}, t)}{\partial t} \tag{6}$$

with respect to the small parameter v. In the zero-order approximation, the transitions between adiabatic states $\varphi_N(\boldsymbol{r}, F)$, defined by

$$H(F)\varphi_N(\boldsymbol{r}, F) = E_N(F)\varphi_N(\boldsymbol{r}, F), \tag{7}$$

are absent. The asymptotic analysis [4] shows that the probability of the inelastic transition between two adiabatic states $|N\rangle$ and $|N'\rangle$ is exponentially small when $v \to 0$ and results from the analytic continuation of the zero-order solution

$$\psi(\boldsymbol{r}, t) = \exp\left[\mathrm{i}\int^{t} E_N(F(vt'))\,\mathrm{d}t'\right]\varphi_N(\boldsymbol{r}, F(vt)) \tag{8}$$

along a contour L in the complex t-plane that enclosed the complex branch point $t_c = T(F_c)/v$, where $T(F)$ is the inverse function to $F(T)$ and $T = vt$. After encompassing the branch point t_c and returning back to the real t-axis, the system finds itself in the state $|N'\rangle$. Since the adiabatic wavefunction attains a singular normalization factor $\varphi_N(\boldsymbol{r}, F) \sim (F - F_c)^{-1/4}$, after returning back to the real t-axis (or F-axis), $\varphi_N(\boldsymbol{r}, F)$ goes over into the wavefunction $\varphi_{N'}(\boldsymbol{r}, F)$ with a phase factor $\gamma = \pm\pi/2$ (the sign depends on direction of encircling). The phase γ was called the 'topological' phase [14] because it is related to the topological properties of the Riemann energy surface.

The system passes the hidden-crossing region twice: during the increasing and decreasing stages of the pulse. Therefore, there are two topologically independent contours, L_1 and L_2, leading to the same final state $|N'\rangle$. The direction of encircling F_c along L_1 and L_2 are opposite to each other and the resulting topological phases have opposite signs. Taking this into account, as well as the superposition principle and unitarity condition, the probability of transition after two passages of the hidden crossing reads [3, 14]

$$P_{NN'} = 4\,\mathrm{e}^{-2\tau\xi_{NN'}}(1 - \mathrm{e}^{-2\tau\xi_{NN'}})\sin^2(\tau\chi_{NN'}) \tag{9}$$

where

$$\xi_{NN'} = \left|\mathrm{Im}\int_{L_1} E_N(F(T))\,\mathrm{d}T\right| = \left|\mathrm{Im}\int_{L_2} E_N(F(T))\,\mathrm{d}T\right| \tag{10}$$

$$\chi_{NN'} = \frac{1}{2}\,\mathrm{Re}\left[\int_{L_1} E_N(F(T))\,\mathrm{d}T - \int_{L_2} E_N(F(T))\,\mathrm{d}T\right]. \tag{11}$$

The expression (9) gives the equidistant oscillations with respect to the duration of the pulse $\tau = 1/v$ which is due to the interference between populations of the final state $|N'\rangle$ along two independent contours L_1 and L_2.

The population of the second excited state takes place in two steps: first, the transition from the ground state to the first excited state via the hidden crossing at negative time $t_{12}^{(-)}$ and second, double transition via hidden crossing at $t_{23}^{(\pm)}$ lying between the branch points $t_{12}^{(\pm)}$. As a result, we obtain the following expression:

$$P_{13} = 4\exp(-2\tau(\xi_{12} + \xi_{23}))(1 - \exp(-2\tau\xi_{23}))\sin^2(\tau\chi_{23}). \tag{12}$$

The adiabatic approximation is valid for pulse duration longer than the typical period of rotation of H_2O which is $T_{\mathrm{rot}} \sim 10^4$ au.

4. Transitions between rotational states

For the Gaussian pulse

$$\boldsymbol{F}(t) = \boldsymbol{F}_0\exp(-t^2/\tau^2), \tag{13}$$

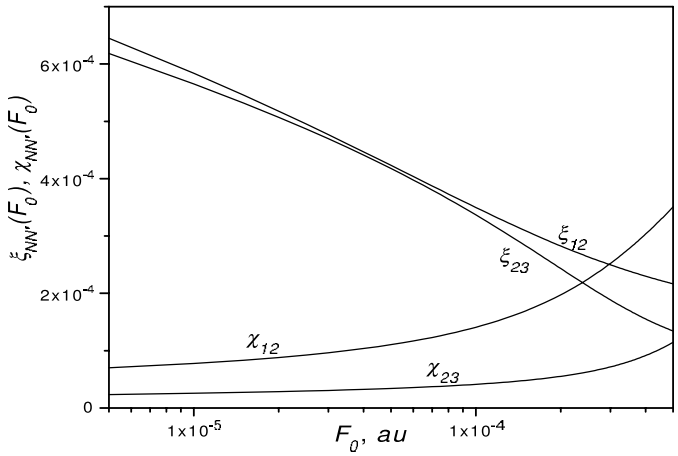

Figure 2. Parameters $\xi_{NN'}$ and $\chi_{NN'}$ for the coupling between the ground and first excited states (ξ_{12}, χ_{12}) and between the first and second excited states (ξ_{23}, χ_{23}) as a function of F_0.

the functions $\xi_{NN'}(F_0)$ and $\chi_{NN'}(F_0)$ take the form

$$\xi_{NN'}(F_0) = \left| \mathrm{Im} \int_{F_0}^{F_{NN'}} \frac{[E_{NM}(F) - E_{N'M}(F)]\,\mathrm{d}F}{2F\sqrt{\ln F_0 - \ln F}} \right|, \tag{14}$$

$$\chi_{NN'}(F_0) = \left| \mathrm{Re} \int_{F_0}^{F_{NN'}} \frac{[E_{NM}(F) - E_{N'M}(F)]\,\mathrm{d}F}{2F\sqrt{\ln F_0 - \ln F}} \right|, \tag{15}$$

where $\boldsymbol{F}_0$ is the amplitude and $\tau = 1/v$ is the duration of the pulse, and $F_{NN'}$ is the position of the complex branch point. These quantities completely determine the transition probability between N and N' states (see equations (9), and (12)). Figure 2 shows the F_0 dependence of $\xi_{NN'}(F_0)$ and $\chi_{NN'}(F_0)$ for transitions from the ground state to the first excited state and from the first to the second excited state. As one can see from figure 2, $\xi_{NN'}(F_0)$ logarithmically diverges when $F_0 \to 0$ as $|\Delta E_{NN'}\,\mathrm{Im}\sqrt{\ln(F_0/F_{NN'})}|$, where ΔE_{nm} is the energy splitting at $F = 0$. This provides a zero transition probability when the pulse amplitude goes to zero.

In figure 3, the comparison between the adiabatic result (dashed lines) and the *ab initio* numerical calculation (solid lines) of the non-stationary Schrödinger equation

$$\left[AJ_a^2 + BJ_b^2 + CJ_c^2 - \boldsymbol{F}_0 \exp\left(-\frac{t^2}{\tau^2}\right) \boldsymbol{d} \right] \psi(\boldsymbol{r}, t) = \mathrm{i}\frac{\partial \psi(\boldsymbol{r}, t)}{\partial t} \tag{16}$$

is given. The *ab initio* calculation was performed in the basis of normalized D-functions $|JKM\rangle$. The numerical accuracy of these results is better than six significant digits in the probabilities. In fact, due to the small transition probabilities the convergence is achieved even for rather small ($J_{\max} = 4$) size of the basis in equation (16). Figure 3 demonstrates good agreement between the adiabatic and exact calculations, especially for longer pulses. First of all, the *ab initio* calculation reproduces the regular equidistant (with respect to τ) oscillations which are impossible to explain from the conventional diagram of adiabatic energy curve in figure 1(a). These oscillations can be explained within the hidden-crossing theory only. For instance, the period of the oscillation in the population of the second excited state is three times longer than the period in the population of the first excited state due to the three times smaller phase factor χ_{nm} (see figure 2). Note that the arguments of the exponent and sine

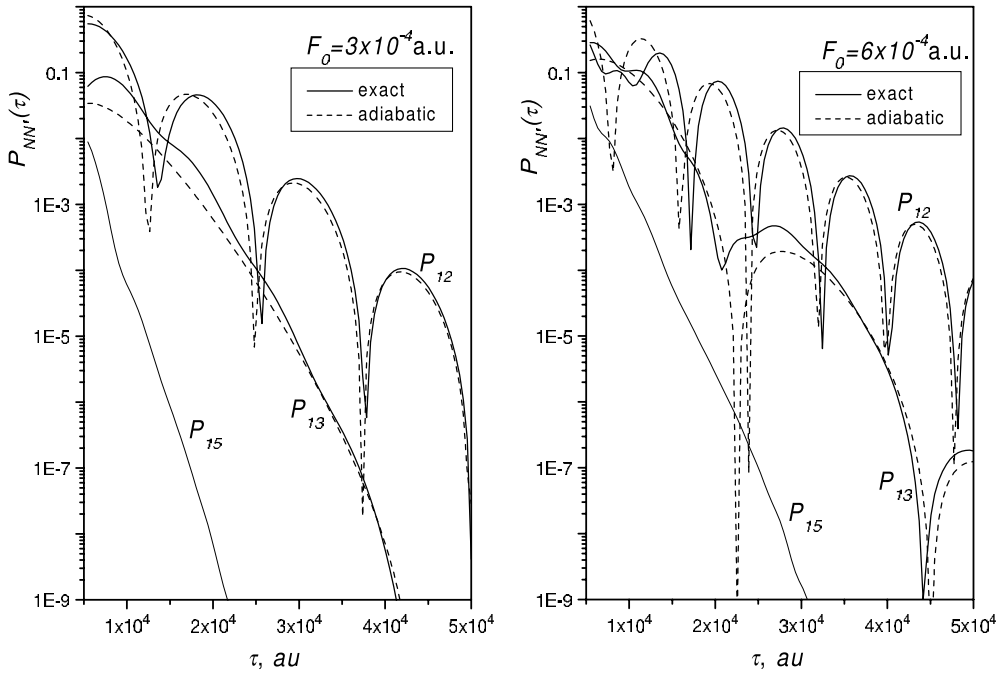

Figure 3. Probability of transitions from the ground state to the excited states $P_{NN'}$ at the different amplitudes of the pulse F_0.

functions in equation (12) are linear functions of the pulse duration τ. The fourth state is not populated because it belongs to another (specific for $M = 0$) symmetry with $(-)$ parity [6].

5. Concluding remarks

Let us estimate the possibility to observe the predicted interference oscillation structure experimentally. The first excited vibrational energy level lies 1596.5 cm^{-1} above the ground state [12], i.e. below the temperature 2300 K (1 cm^{-1} = 1.44 K) the vibrational states are not excited and our calculations are almost exact. Since the atomic unit of time is 2.42×10^{-17} s and the atomic unit of electric field is equal to 5.14×10^9 V cm^{-1}, the pulse parameters needed to observe the adiabatic oscillations are quite attainable and reliable: the duration of the pulse should be about 1 ps and the electric field should be about 10^6 V cm^{-1}.

The adiabatic approximation used here is not intended to produce specific data only, but, what is more important, to demonstrate that it is a powerful tool to understand the origin of certain physical effects (in our case it is the oscillation in the inelastic probability) and to make some general predictions.

Acknowledgments

This work was partially supported by a grant-in-aid for Scientific Research, grant nos 13440182 and 15002011 from the Ministry MEXT of Japan. One of us (EAS) thanks the Institute for Molecular Science for visiting professorship during 2002-2003.

References

[1] Dimitrovski D, Pop-Jordanov J, Pop-Jordanova N and Solov'ev 1998 *Contrib. Sec. Math. Tech. Sci. MANU* **19** 35
Dimitrovski D, Pop-Jordanov J, Pop-Jordanova N and Solov'ev 2004 *Inf. Sci.* at press
[2] Solov'ev E A 1998 *Phys. Lett.* A **249** 74
[3] Stueckelberg E C G 1932 *Helv. Phys. Acta* **5** 369
[4] Solov'ev E A 1989 *Sov. Phys.—Usp.* **32** 228
[5] Grozdanov T P and McCarroll R 1996 *Z. Phys.* D **38** 45
[6] Sakimoto K 1982 *Chem. Phys.* **68** 155
[7] Tennyson J, Zobov N F, Williamson R, Polyansky O L and Bernath P F 2001 *J. Phys. Chem. Ref. Data* **30** 735
[8] Hellwege K H and Hellwege A M 1974 *Landolt–Bornstein, New Series II/6* (Berlin: Springer)
[9] Rose M E 1957 *Elementary Theory of Angular Momentum* (New York: Wiley)
[10] Polyansky O L, Csaszar A G, Shirin S V, Zobov N F, Barletta P, Tennyson J, Schwenke D W and Knowles P J 2003 *Science* **299** 539
[11] Duke A 1973 *Chem. Phys. Lett.* **21** 275
[12] Whitehead R J and Handy N C 1975 *J. Mol. Spectrosc.* **55** 356
[13] Leitner D M, Hunter J E III, Natanson G A and Berry R S 1991 *J. Chem. Phys.* **94** 5917
[14] Janev R K, Pop-Jordanov J and Solov'ev E A 1997 *J. Phys. B: At. Mol. Opt. Phys.* **30** L353